Equilibrium and Transient State Spectrophotometric Studies of the Mechanism of Reduction of the Flavoprotein Domain of P450BM-3[†]

Irina Sevrioukova,[‡] Catherine Shaffer,[§] David P. Ballou,[§] and Julian A. Peterson*,[‡]

Department of Biochemistry, The University of Texas Southwestern Medical Center at Dallas, Dallas, Texas 75235-9038, and Department of Biological Chemistry, The University of Michigan, Ann Arbor, Michigan 48109-0606

Received January 10, 1996; Revised Manuscript Received March 19, 1996[⊗]

ABSTRACT: The flavoprotein domain of P450BM-3 (BMR), which is functionally analogous to eukaryotic NADPH−P450 oxidoreductases, contains both FAD and FMN. When BMR is titrated with NADPH or sodium dithionite under anaerobic conditions, addition of 2 electron equivalents per mole of BMR results in the reduction of the high potential flavin (FMN) without the accumulation of semiquinone intermediates. Additional sodium dithionite first produces some neutral, blue flavin semiquinone radical and, finally, fully reduced $FADH_2$. During reduction with NADPH, an absorbance increase characteristic of the formation of a flavin−pyridine nucleotide charge-transfer complex was observed only during the addition of the second mole of NADPH per mole of BMR. On the basis of these results, we conclude that the midpoint reduction potential for the FMN semiquinone/$FMNH_2$ couple is more positive than that for FMN/FMN semiquinone. The kinetics of reduction of BMR with NADPH were studied by stopped-flow spectrophotometry. With a 1:1 ratio of NADPH to BMR, the absorbance changes can be fit to five consecutive first order reactions with rate constants of 350 s^{-1}, 130 s^{-1}, 27 s^{-1}, 2.3 s^{-1}, and 0.05 s^{-1}. These reactions are most probably the following: (a) complex formation between BMR and NADPH; (b) reduction of FAD with formation of the $NADP^+$−$FADH^-$ charge-transfer complex; (c) transfer of the first electron from $FADH^-$ to FMN to form an anionic, red FMN semiquinone leaving the FAD as the neutral, blue semiquinone. Precise identification of intermediates beyond this point is difficult. In the presence of a 10-fold molar excess of NADPH, the absorbance changes and rate constants are somewhat different due to the formation of several additional reduced species of BMR. The rate of the first step increases, confirming that this is the formation of the NADPH−BMR complex. Our results indicate that the kinetic and thermodynamic control of the flavins in BMR is significantly different from that in microsomal P450 reductase. The low potential of the anionic FMN semiquinone can be utilized to reduce the P450 heme. When the anionic semiquinone becomes protonated, its potential becomes more positive and it is readily reduced to $FMNH_2$, which is not capable of reducing P450.

Monooxygenation reactions catalyzed by the P450 gene superfamily of proteins require the input of two electrons. The source of electrons is usually reduced pyridine nucleotide, and the electrons are transferred to the P450 *via* electron transfer partners. *Class I* P450s utilize two electron transfer proteins, a flavoprotein reductase and an iron sulfur protein, while *Class II* P450s utilize only a single reductase that contains two flavins. Microsomal NADPH−P450 reductase is a complex, multidomain protein containing an NADPH-binding domain with tightly bound FAD, and a flavodoxin-like domain (Porter & Kasper, 1986; Smith et al., 1994) with tightly bound FMN.

Studies with the native and FMN-depleted forms of microsomal NADPH−P450 reductase have established the FAD moiety as the acceptor of the hydride from NADPH, whereas the FMN moiety donates electrons to P450, cytochrome *c*, and cytochrome b_5 (Vermilion & Coon, 1978a; Vermilion et al., 1981; Nisimoto & Shibata, 1982). In addition to the separate electron transfer roles, each flavin has distinctive reactivity toward oxygen. When fully reduced enzyme is exposed to oxygen, the $FADH_2$ is rapidly and completely oxidized, whereas the $FMNH_2$ is oxidized rapidly only as far as the one-electron-reduced state, forming an air-stable neutral, blue semiquinone, $FMNH^\bullet$ (Vermilion & Coon, 1978a,b; Iyanagi & Mason, 1973; Iyanagi et al., 1978, 1974, 1981; Yasukochi et al., 1979; Strobel et al., 1980). The air-stable semiquinone form of microsomal NADPH−P450 reductase, 1 e^- in Scheme 1, does not efficiently reduce $P450_{LM}$[1] (Oprian et al., 1979) or cytochrome *c*, (Masters et

[†] This work was supported in part by research grants from the National Institutes of Health to J.A.P. (GM50858) and to D.P.B. (GM20877).

* Please address all correspondence to this author at the Department of Biochemistry, The University of Texas Southwestern Medical Center at Dallas, Dallas, TX 75235-9038. Tel: (214) 648-2361; FAX: (214) 648-8856; E-Mail: peters01@UTSW.SWMED.EDU; dballou@UMICH.EDU.

[‡] The University of Texas Southwestern Medical Center at Dallas.

[§] The University of Michigan.

[⊗] Abstract published in *Advance ACS Abstracts,* May 15, 1996.

[1] Abbreviations: $P450_{LM}$, liver microsomal P450; P450BM-3, the soluble P450 isolated from *Bacillus megaterium* (the product of the CYP102 gene); BMR, the recombinantly expressed flavoprotein domain (reductase) of P450BM-3; $P450_{cam}$, the soluble P450 isolated from *Pseudomonas putida* (the product of the CYP101 gene); PCA, protocatechuic acid; PCD, protocatechuic acid dioxygenase; MOPS, 4-morpholinopropanesulfonic acid; FMN (FAD), oxidized form of FMN (FAD); $FMNH^\bullet$ ($FADH^\bullet$), the neutral, blue semiquinone of FMN (FAD); $FMN^{\bullet-}$, the anionic red semiquinone of FMN; $FMNH_2$ ($FADH_2$), the fully reduced form of FMN (FAD); $FMNH^-$ ($FADH^-$), the anionic fully reduced form of FMN (FAD). It should be noted that the fully reduced forms of flavin in most flavoproteins have been shown to be the anionic species (Muller, 1991).

S0006-2960(96)00060-8 CCC: $12.00

Scheme 1

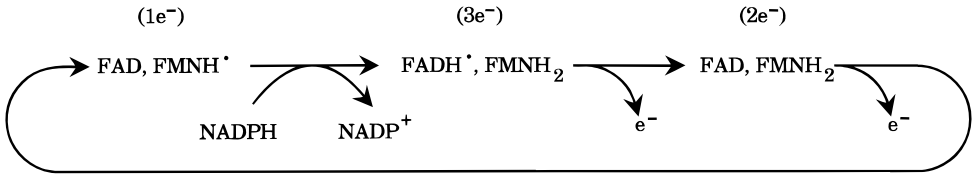

al., 1965) in the absence of additional reducing equivalents. However, this one-electron-reduced form has been proposed to be an intermediate during enzyme catalysis (Iyanagi et al., 1981), with the sum of the electrons on the flavins cycling between 1 e^- and 3 e^- states during turnover as electrons are donated to acceptors via the reactions shown in Scheme 1.

Potentiometric titrations have established the reduction potentials of each flavin half-reaction for the native microsomal NADPH−P450 reductase (Vermilion & Coon, 1978a; Iyanagi et al., 1974). Although the kinetics and thermodynamics of the transient intermediates in the catalytic cycle of this enzyme have been reported, there is still not general agreement on the precise catalytic mechanism (Strobel et al., 1970; Tamburini et al., 1984; Backes & Reker-Backes, 1988).

The bacterial, fatty acid ω-hydroxylase P450 system, P450BM-3, is functionally analogous to the microsomal P450 system, including the transfer of electrons to the heme from NADPH *via* FAD and FMN (Miura & Fulco, 1974). P450BM-3 is a soluble, catalytically self-sufficient single polypeptide ($M_r \cong 119\,000$) containing heme, FAD, and FMN in a stoichiometry of 1:1:1, respectively (Narhi & Fulco, 1986). The turnover number of purified P450BM-3, in the monooxygenation of palmitic acid, is 27 s^{-1} at 25 °C (Narhi & Fulco, 1986; Boddupalli et al., 1990), which is approximately equal to that of $P450_{cam}$ under similar conditions (Katagiri et al., 1968; Peterson & Mock, 1975) and 25−1000 times greater than those of mammalian P450 systems. The flavoprotein domain (BMR) of P450BM-3 has been expressed independently (Oster et al., 1991) and contains both FAD and FMN, in a stoichiometry of 1:1. The flavoprotein domain shares 33% and 40% amino acid sequence identity with rabbit and rat hepatic microsomal NADPH−P450 reductases, respectively, with highly conserved segments that are likely to be involved in the binding of the flavins and pyridine nucleotides (Ruettinger et al., 1989). Sequence analysis indicates that BMR, like microsomal NADPH−P450 oxidoreductases, has a discrete multidomain structure, with an amino-terminal FMN-binding domain and a carboxyl-terminal FAD- and NADPH-binding domain (Porter, 1991; Oster et al., 1991). Based on sequence analysis, these structures have been described as common to the FNR (ferredoxin $NADP^+$ reductase) family of flavoprotein oxidoreductases, which comprises FNR, phthalate dioxygenase reductase, cytochrome b_5 reductase, NO synthase, sulfite reductase, nitrate reductase, and others (Correll et al., 1992; Karplus et al., 1991; Andrews et al., 1992). X-ray structures of FNR (Karplus et al., 1991), phthalate dioxygenase reductase (Correll et al., 1993), cytochrome b_5 reductase (Takano et al. 1993), and nitrate reductase (Lu et al., 1994) confirm that these proteins are structurally related.

The reductive titration of P450BM-3 with sodium dithionite, in the presence of palmitic acid and carbon monoxide, was complete with the addition of the expected 5 electron equivalents (Peterson & Boddupalli, 1992). The intermediate spectra indicate that the heme iron is reduced first, followed by the flavin residues. Titration of the protein with the physiological reductant, NADPH, was performed under an atmosphere of carbon monoxide, and the heme iron was reduced first, followed by the flavins; however, the flavins were not completely reduced under these conditions. Under an atmosphere of argon and in the absence of carbon monoxide, one of the flavin groups was reduced to the hydroquinone form prior to the reduction of the heme group, leading to the conclusion that the redox potential of this flavin is more positive than that of the heme.

In the current paper, in order to clarify whether the differences in the electron donor/acceptor properties of the reductase domain are intrinsic properties of this multidomain protein or a consequence of interdomain interactions, spectrophotometric titrations and analysis of the kinetics of reduction of the flavoprotein domain of P450BM-3 with sodium dithionite and NADPH were performed. On the basis of a multiwavelength analysis by stopped-flow spectrophotometry, a model was found that would predict the spectral course of each phase of the reaction of NADPH with BMR under anaerobic conditions. Experiments with the holoenzyme, P450BM-3, have shown that the rate constant of the first electron transfer to the heme correlates with the rate constant of the formation of the red, anionic $FMN^{\bullet -}$. These results highlight some of the similarities and differences between BMR and mammalian microsomal NADPH−P450 reductase.

MATERIALS AND METHODS

Materials. Cytochrome *c*, NADPH, $NADP^+$, protocatechuic acid (PCA), MOPS, and Trizma base were obtained from Sigma. Sodium dithionite was obtained from Hardman and Holden, Ltd., Manchester, England. Arachidonic acid was obtained from NuChek Prep, Inc. Protocatechuate 3,4-dioxygenase (PCD) was prepared according to a published procedure (Bull & Ballou, 1981). All other reagents were purchased from commercial sources and were of the purest grades available.

Experimental Procedures. Protein concentrations were estimated (Lowry et al., 1951) using bovine serum albumin as a standard. P450BM-3 and BMR were purified by published procedures (Boddupalli et al., 1990; Oster et al., 1991). The concentration of BMR was determined at the wavelength of maximal absorbance in the 450 nm region using the extinction coefficient for purified microsomal NADPH−P450 reductase, 21.4 mM^{-1} cm^{-1} (French & Coon, 1979). The concentration of P450BM-3 was determined by conventional difference spectrophotometry with the sodium dithionite reduced enzyme in the reference cuvette and the reduced enzyme under a carbon monoxide atmosphere in the sample cuvette. The difference in absorbance between 450 and 490 nm was measured, and the difference extinction

coefficient of 91 $mM^{-1}cm^{-1}$ for this wavelength pair was used (Omura & Sato, 1964).

The samples for both optical absorbance spectroscopy and stopped-flow spectrophotometry were made oxygen free by repeated evacuation and flushing with prepurified argon as previously described (Peterson, 1971; Peterson et al., 1977). The titrants were prepared in anaerobic buffer and standardized. Sodium dithionite was standardized by titrating a solution of cytochrome *c*, while NADPH was standardized by diluting the reagent into buffer and measuring the absorbance at 340 nm versus a buffer blank using the extinction coefficient, 6.22 mM^{-1} cm^{-1}. The reaction mixtures contained 50 mM MOPS buffer, pH 7.4, 40−44 μM BMR, and an oxygen-scavenging system consisting of 1 μM PCD and 100 μM PCA (Bull & Ballou, 1981). All manipulations of the titrator assembly were performed in a glovebag that was continuously flushed with prepurified nitrogen to minimize contamination with oxygen. Absorbance spectra were recorded at 20 °C with an IBM Model 9420 UV/visible spectrophotometer. Following the addition of each aliquot of titrant, the reaction mixture was permitted to stand at room temperature until no further absorbance changes occurred, usually less than 10 min.

Stopped-flow spectrophotometric studies were performed with a Hi-Tech Scientific Co. Model SF-61 stopped-flow spectrophotometer. All kinetic experiments were performed at 4 °C in anaerobic, filtered 50 mM MOPS buffer, pH 7.4, containing 1 μM PCD and 100 μM PCA as an oxygen-scavenging system (Bull & Ballou, 1981). Samples containing PCD were vacuum gas exchanged in glass tonometers and overlaid with 2 psi of argon; then PCA was added from a side arm of the tonometer.

In the case of reduction of BMR, one syringe of the apparatus contained a solution of 42−44 μM BMR, and the other contained either 40 or 450 μM NADPH. Equal volumes of the two solutions were mixed in the mixing chamber (40−45 μL per shot, 2 ms dead time). The stopped-flow instrument was set up for interconversion between single wavelength, photomultiplier mode and diode array mode, making both forms of data collection accessible in a single experiment. Single wavelength data were collected at 380, 456, 510, 550, and 750 nm logarithmically with respect to time using a MacADIOS interface board equipped with a 16-bit analog-to-digital converter. Data collection was controlled with KISS software and hardware from Kinetic Instruments, Inc., installed in a Macintosh IIcx. When operated in the diode array detection mode, each spectrum was recorded in a period of 1.23 ms with a variable interval between spectra. Diode array data were collected using Hi-Tech Scientific Co. hardware and software installed in a 66 MHz DX2 Gateway 2000 computer.

In the case of the reduction of the holoenzyme of P450BM-3, different combinations of 3.8 μM P450BM-3, 4 or 400 μM NADPH, and 50 μM arachidonic acid in the buffers saturated with argon or carbon monoxide were used for the experiments. The absorbance change at 450 nm was recorded as a function of logarithmic time.

The method of analysis of the kinetic data from these experiments involved data fitting to analytical expressions using a consecutive exponential fitting routine based on the Marquardt−Levenberg algorithm (Bevington, 1969). The data were fit to the equations for five irreversible exponential steps as described in the text. The data fitting routines are built-in features of Program A for PC-compatible computers; this program for analyzing and collecting data was written in D. Ballou's laboratory by Joel Dinvero, Chung-Jen Chiu, and Rong Chang.

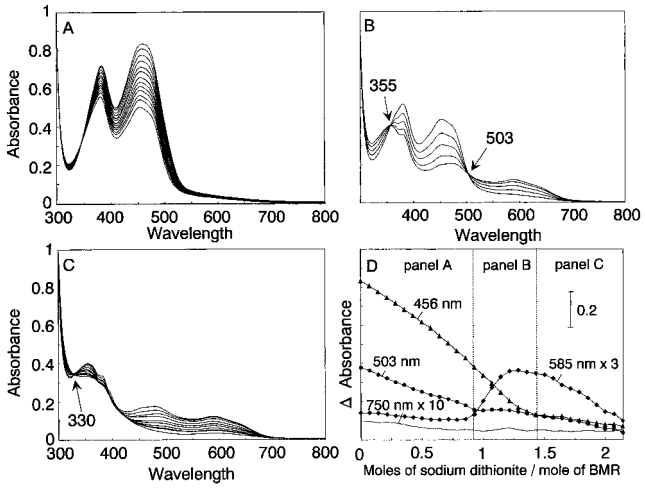

FIGURE 1: Anaerobic titration of oxidized BMR with sodium dithionite. BMR (40 μM) in 50 mM MOPS buffer, pH 7.4, was titrated at 5 °C in the presence of methylviologen (2 μM) with sodium dithionite (4.7 mM). The absorbance spectra have been corrected for dilution. Panels A, B, and C represent a single continuous titration of enzyme. Curves are separated in the three graphs to show individual sets of isosbestic points occurring during the titration. Panel D is a plot of absorbance changes at 456 (—▲—), 503 (—●—), 585 (—♦—), and 750 (—) nm as a function of sodium dithionite added.

RESULTS

Anaerobic Reduction of BMR with Sodium Dithionite. Absorbance changes associated with the anaerobic titration of BMR with sodium dithionite are shown in Figure 1A−C, and changes for selected wavelengths are replotted versus the number of moles of sodium dithionite added per mole of BMR in panel D of this figure. Sodium dithionite reduction took place in three spectrally distinct phases. In the first phase, 1 mol of sodium dithionite was consumed per mole of BMR (2 electron equivalents per 2 flavins) (Figure 1A,D). During this phase of the titration, the absorbance between 345 and 800 nm decreased without the appearance of additional absorbance bands. This indicates that there is no accumulation of the neutral, blue semiquinone form of the flavins. The reduction by sodium dithionite is *via* the donation of one electron at a time through an $SO_2^{\bullet-}$ radical species (Mayhew & Massey, 1973; Lambeth & Palmer, 1973); therefore, a flavin semiquinone must have been formed transiently, and the absence of observable semiquinone implies that the second electron is taken up more easily than the first. Whether this is by direct reduction by sodium dithionite or by intermolecular disproportionation of the flavins is not known at present. Thus, at the end of the first phase, which represents about 50% reduction of the enzyme, the spectrum resembled a mixture composed primarily of oxidized and two-electron-reduced flavin with, presumably, the FMN component reduced and the FAD oxidized.

Upon the further addition of 0.5 mol of sodium dithionite (a total of 3 electron equivalents per mole of BMR), there was an increase of absorbance at 585 nm and isosbestic points appeared at 355 and 503 nm (Figure 1B,D). During

this phase, the remaining oxidized flavin (FAD) became reduced to the neutral, blue semiquinone state. An additional 0.5 mol of sodium dithionite per mole of BMR caused an absorbance decrease from 400 to 700 nm (Figure 1C) and is shown at 456 and 585 nm (Figure 1D). The spectral changes observed in the final phase were isosbestic at 330 nm and represent reduction of a neutral, blue flavin semiquinone to the hydroquinone. As seen in this figure, there was no absorbance increase in the long wavelength regions (>700 nm).

Anaerobic Reduction of BMR with NADPH. There were three discrete phases in the titration of BMR with NADPH, as judged from the plot of absorbance change versus NADPH added (Figure 2D). In the first phase of this titration, the addition of 1 mol of NADPH (2 electron equivalents) per mole of BMR was spectrally very similar to the titration with 1 mol of sodium dithionite. An absorbance decrease was observed at 456 nm without an increase in absorbance either at 585 nm or in the longer wavelength regions. There was an isosbestic point at 352 nm during this phase of the titration. In the second phase, approximately 1.5 additional mol of NADPH per mole of enzyme produced an increase at 585 nm, indicative of the formation of a neutral, blue flavin semiquinone; however, there were also absorbance changes in this region due to the formation of a charge-transfer complex between $NADP^+$ and the FAD. The long wavelength absorbance (750 nm in the plot in Figure 2D) is a characteristic feature of charge-transfer interactions between $NADP^+$ and $FADH^-$ (Massey & Palmer, 1962; Massey & Ghisla, 1974). A comparison of the NADPH titration spectra with the sodium dithionite titration spectra shows that one of the isosbestic points observed in this phase of the titration was shifted from 503 to 516 nm; this shift is probably due to the contribution of the charge-transfer complex. The third phase (panel C) began after addition of approximately 5 electron equivalents (2.5 mol of NADPH/mol of BMR). There were only small changes in the flavoprotein spectrum, while an increase in absorbance around 340 nm indicated that unreacted NADPH was accumulating. In addition, an isosbestic point appeared at 510 nm.

$NADP^+$ is a competitive inhibitor of microsomal NADPH oxidoreductases (Williams & Kamin, 1962). Thus, the reduction of BMR with NADPH was compared in the absence and presence of a 10-fold excess of $NADP^+$. The presence of $NADP^+$ did not affect the initial phase of titration, but did result in requiring a larger concentration of NADPH to achieve maximal reduction of the flavins (data not shown), indicating that the effect is primarily thermodynamic. In a separate experiment, BMR was anaerobically titrated with sodium dithionite until more than 2 electron equivalents per flavin had been added (corresponding to complete reduction of the enzyme). At this point, a 10-fold excess of $NADP^+$ was added anaerobically. The absorbance increased over the range 340−800 nm, indicating partial reoxidation of BMR with formation of NADPH, neutral, blue flavin semiquinone, and a charge-transfer complex between oxidized pyridine nucleotide and reduced flavin. When a 100-fold excess of $NADP^+$ was added to the sodium dithionite reduced enzyme, the spectrum resembled two-electron-reduced BMR.

Reoxidation of BMR. Because of the difference in the titration behavior of BMR and microsomal NADPH−P450 reductase, we examined the reaction of reduced BMR in the presence of molecular oxygen. Absorbance spectra (not shown) indicate that BMR becomes fully oxidized without forming the air-stable, neutral, blue semiquinone that has been observed with microsomal NADPH−P450 reductase (Vermilion & Coon, 1978b; Iyanagi et al., 1981; Iyanagi & Mason, 1973; Masters et al., 1975). To determine the rate of this oxidation, BMR that had been reduced with a 4-fold molar excess of NADPH as described in Figure 2 was mixed with oxygen-saturated buffer, and the oxidation was followed spectrophotometrically at 456 and 585 nm. There was an initial lag period during which the excess NADPH was oxidized, followed by a rapid loss of the absorbance at 585 nm and a gain in absorbance at 456 nm. These rapid changes were followed by a slower appearance of absorbance at 456 nm until the initial absorbance had been recovered. The rate constants for the fast and slow reoxidation reactions at room temperature were approximately 0.7 and 0.06 min^{-1}, respectively, and probably will vary as a function of oxygen concentration. The mechanism of reoxidation of the flavins of BMR is not clear at the present time.

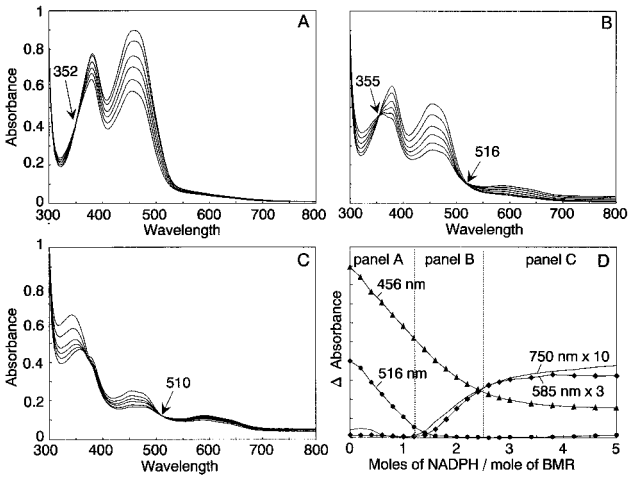

FIGURE 2: Anaerobic titration of oxidized BMR with NADPH. BMR (40 μM) in 50 mM MOPS buffer, pH 7.4, was titrated at 5 °C with NADPH (4 mM). The absorbance spectra have been corrected for dilution. Panels A, B, and C represent a single continuous titration of enzyme. Curves are separated in the figure to show three individual sets of isosbestic points occurring during the titration. Panel D is a plot of absorbance changes at 456 (—▲—), 516 (—●—), 585 (—♦—), and 750 (—) nm as a function of NADPH added.

Kinetics of Reduction of BMR. The reaction of NADPH with BMR was examined under anaerobic conditions by stopped-flow spectrophotometry (Figures 3 and 4). To permit observation of all phases of the reaction on a single time scale, logarithmic *x*-coordinates are used for plotting the kinetic curves. The wavelengths shown from these studies are as follows: 380 nm, to monitor the anionic, red flavin semiquinone; 456 nm, to follow the overall reduction of flavin (FAD or FMN); 510 nm, to discriminate between formation of the fully reduced flavin and flavin semiquinone (since the blue and red (neutral and anionic) semiquinone forms of flavin are almost isosbestic at this wavelength); 550 nm, to monitor the neutral, blue flavin semiquinone; and 750 nm, to follow charge-transfer complexes with pyridine nucleotides. Note that none of these wavelengths is completely specific for a single form because of the broad overlapping nature of flavin absorbance spectra.

The spectrophotometric traces in Figure 3 were obtained from experiments at 5 °C in which BMR was rapidly mixed

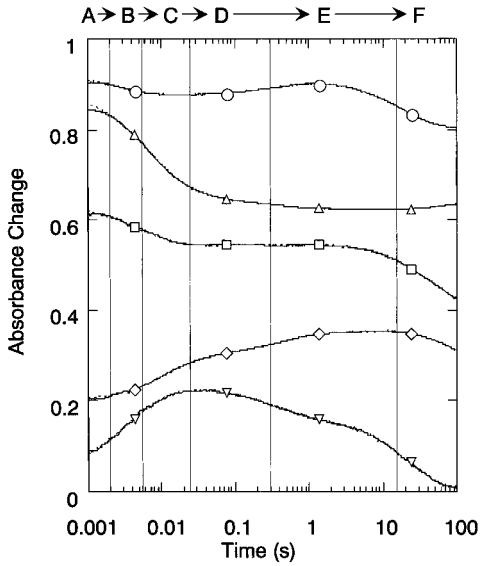

FIGURE 3: Kinetic absorbance changes during the reduction of BMR by a 1:1 ratio of NADPH to BMR. BMR (40 μM) in 50 mM MOPS buffer, pH 7.4, was mixed with an equal volume of NADPH (40 μM) in the stopped-flow spectrophotometer. The final concentrations of reactants were 20 μM. The data represent the average of 3−5 experimental determinations and are offset and expanded to promote visualization. The data were offset by 0.5 at 380 nm (—○—), by 0.40 at 456 nm (—△—), multiplied by 5 and offset by −0.65 at 510 nm (—□—), multiplied by 5 with no offset at 550 nm (—◇—), and multiplied by 10 with a −0.025 offset at 750 nm (—▽—). In each experiment, the dashed line represents the calculated absorbance change based on the rate constants given in Scheme 1 for the reaction shown at the top of the figure. The vertical lines show the position of $t_{1/2}$ for each of the steps in the reaction. The data are most consistent with the following: A = [FAD, FMN]; B = [NADPH, FAD, FMN]; C = [$NADP^+$, $FADH^-$, FMN]; D = [$NADP^+$, $FADH^•$, $FMN^{•-}$]; E = [$FADH^•$, $FMNH^•$] + [FAD, $FMNH_2$]; and F = [FAD, $FMNH^-$].

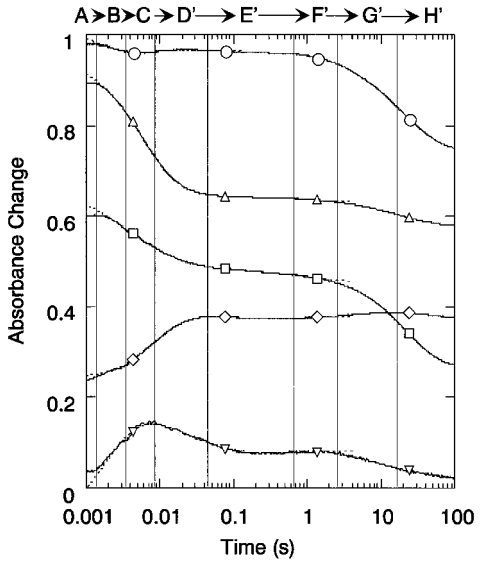

FIGURE 4: Kinetic absorbance changes during the reduction of BMR by a 10:1 ratio of NADPH to BMR. The conditions were the same as in Figure 3 except that NADPH was 400 μM before mixing. The data represent the averages of 3−5 experimental determinations and are offset and expanded to promote visualization. The data were offset by 0.35 at 380 nm (—○—), by 0.5 at 456 nm (—△—), multiplied by 5 and offset by −0.20 at 510 nm (—□—), multiplied by 5 with no offset at 550 nm (—◇—), and multiplied by 10 with a −0.2 offset at 750 nm (—▽—). In each experiment, the dashed line represents the calculated absorbance change based on the rate constants given in Scheme 3. The vertical lines show the $t_{1/2}$ for each of the intermediates of the reaction: A = [FAD, FMN]; B = [NADPH, FAD, FMN]; C = [$NADP^+$, $FADH^-$, FMN]; D′ = [$NADP^+$(H), $FADH^•$, $FMN^{•-}$]; E′ = [NADPH, $FADH^•$, $FMNH^•$]; F′ = [FAD, $FMNH^-$]; G′ = [$NADP^+$, $FADH^-$, $FMNH^-$]; and H′ = [$NADP^+$(H), $FADH^•$, $FMNH^-$].

anaerobically with an equimolar concentration of NADPH (1 mol of NADPH per 2 flavins). The data for these wavelengths, out to about 10 s, can be fit to an equation describing five consecutive first order processes as shown by the dashed theoretical line in each figure. In order to calculate the rate constant for the last phase of the reaction within the interval of 0.1−100 s, the curve fitting for this portion of the data was performed separately. The curves resulting from the calculations for this final phase of the reaction are not shown in the figure. The rate constants for the interconversion of the components are shown in Scheme 2. All wavelengths examined were fit to the rate constants in Scheme 2 by allowing the amplitudes to vary in the Marquardt−Levenberg procedure.

We believe that the first process in Scheme 2 represents NADPH binding to form a charge-transfer complex with the oxidized FAD, and the second represents reduction of the flavin (FAD). Thus, A would represent oxidized, free reductase, and B would represent the [NADPH, FAD, FMN] charge-transfer complex. Because of the rather small absorbance change associated with the first reaction, we do not believe that this absorbance change represents reduction of the flavin. C would represent the [$NADP^+$, $FADH^-$, FMN] charge-transfer complex resulting from hydride transfer from NADPH to FAD. This intermediate was identified by the dramatic loss of absorbance noted at 456 nm indicating flavin reduction. The formation of the charge-transfer complex can be seen by the corresponding increase in absorbance at 750 nm. D would represent [$NADP^+$, $FADH^•$, $FMN^{•-}$], the product of intracomplex electron transfer. This intermediate was identified by the increase in absorbance at 550 nm, between 20 and 500 ms, indicative of the formation of the neutral, blue flavin semiquinone. The presence of the anionic, red flavin semiquinone in this species was inferred from the lack of an absorbance decrease at 380 nm that would have occurred if either flavin had been fully reduced, or if both flavins were in the neutral, blue semiquinone form. For comparison, note the loss of absorbance at 380 nm in Figure 2 during the equilibrium titration of BMR with NADPH, which indicates that only the reduced or neutral, blue semiquinone forms of the flavins accumulate during the titrations. Species E would represent [$FADH^•$, $FMNH^•$], which results from proton transfer to the anionic, red semiquinone. During equilibrium titrations, this species forms and decays before the spectra are recorded and species F is formed, which represents [FAD, $FMNH^-$] resulting from the second intracomplex electron transfer (see Figure 2).

Scheme 2

	A ⟶ B	B ⟶ C	C ⟶ D	D ⟶ E	E ⟶ F
k	350 s^{-1}	130 s^{-1}	27 s^{-1}	2.3 s^{-1}	0.05 s^{-1}
$t_{1/2}$	2 ms	5.3 ms	26 ms	300 ms	14 s

The kinetic curves obtained from the experiments in which BMR was reduced with a 10-fold excess of NADPH are presented in Figure 4. The rate constants for nearly all of the steps are affected by increasing the concentration of NADPH. The absorbance changes for these wavelengths can be fit to a reaction in which there are seven consecutive processes as shown in Scheme 3. It must be remembered

Scheme 3

	A ⟶	B ⟶	C ⟶	D′ ⟶	E′ ⟶	F′ ⟶	G′ ⟶	H′
k	600 s^{-1}	200 s^{-1}	85 s^{-1}	15 s^{-1}	1 s^{-1}	0.3 s^{-1}	0.04 s^{-1}	
$t_{1/2}$	1.2 ms	3.5 ms	8.2 ms	46 ms	690 ms	2.3 s	17.3 s	

that the identification of species, beyond the first several steps, is very difficult; however, the equilibrium titration data presented above have helped in the identification of potential intermediates in this reaction. Within the first 10 ms of the reaction, decreases in absorbance at 456 and 510 nm and increases in absorbance at 550 and 750 nm were observed. This was due to the very rapid formation of a charge-transfer interaction between NADPH and oxidized flavin, followed by the reduction of the FAD moiety to $FADH^-$, which is in a charge-transfer complex with the resultant $NADP^+$. The 750 nm absorbance increase is very fast, $\geq 600\ s^{-1}$, and is complete when about 50% of the change in absorbance at 450 nm has occurred. The hydride transfer from NADPH to FAD has a rate constant of about 200 s^{-1} at 5 °C. The next step in the reaction is somewhat faster than that observed with an equimolar ratio of NADPH to BMR. The small absorbance changes at 380 and the somewhat larger changes at 550 nm indicate that this involves a one-electron transfer process to produce a neutral, blue semiquinone and an anionic, red semiquinone (species D′).

The identification of species beyond D′ is more difficult. The rate constant for the conversion of D′ to E′ is approximately 7-fold larger than the comparable step with equimolar NADPH and enzyme. The loss of absorbance at 750 nm associated with the conversion of D′ to E′ indicates that $NADP^+$ may have dissociated from the enzyme and been replaced by NADPH, giving the species [NADPH, $FADH^\bullet$, $FMN^{\bullet-}$], which formally contains four electrons (two electrons on NADPH and one each on FAD and FMN). The rate of the second electron transfer to FMN (1 s^{-1}) is affected by increasing the NADPH concentration. No significant absorbance changes are observed in this phase. During the next step in the reaction (F′ → G′; 0.3 s^{-1}), there is a small loss in absorbance at 380, 456, 510, and 750 nm. These absorbance changes may represent hydride ion transfer within the complex [NADPH, FAD, $FMNH^-$] to form [$NADP^+$, $FADH^-$, $FMNH^-$]. Recall that equilibrium titrations (Figure 2) have shown that, at the end of the titration ($t \cong 5$ min), the enzyme is reduced by three electrons, which likely resulted from a comproportionation reaction between a molecule of BMR that has been reduced by two electrons (species F′) and a molecule which has been reduced by four electrons (species G′). Thus, the last slow step in the reduction of BMR with an excess of NADPH (0.04 s^{-1}) will be the formation of three-electron-reduced species, [NADPH, $FADH^\bullet$, $FMN^-(H)$].

Stopped-Flow Diode Array Spectrophotometry. Single wavelength, stopped-flow spectrophotometric data are invaluable in accurately determining the rate constants for individual reactions; however, to aid in the identification of the specific chromophores that are the intermediates in the reaction, we have employed diode array, stopped-flow spectrophotometry. Figure 5 shows the reaction of NADPH and BMR mixed in a 1:1 ratio. The first absorbance spectrum recorded at 1.23 ms after mixing (mixing time equals 2 ms; total time of first spectrum equals 3.23 ms; this curve has no symbols) already shows a significant

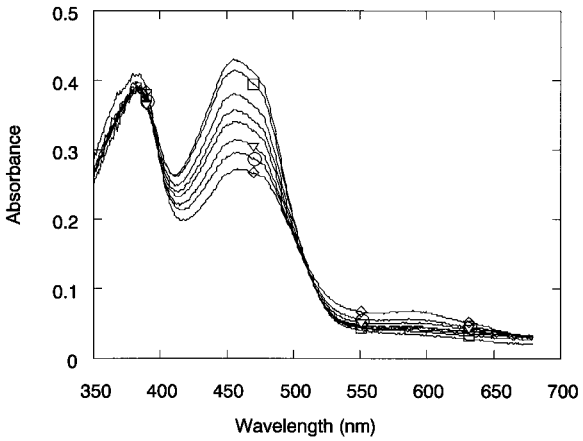

FIGURE 5: Absorbance spectra of BMR at selected time points during the reduction with a 1:1 ratio of NADPH to BMR. The conditions were the same as in Figure 3. The data were obtained with the stopped-flow spectrophotometer using diode array detection. Spectra taken 2.48 ms (—□—), 12.6 ms (—▽—), 23.7 ms (—○—), and 4.0 s (—◇—) after mixing are indicated. The first spectrum was taken 1.23 ms after mixing.

decrease in absorbance in the 456 nm region (ca. 0.05 change) with little or no increase in absorbance in the 585 nm region, in agreement with the single wavelength kinetic data. Although spectra were recorded every 1.23 ms, we have shown only selected time points in this figure. At the end of the first two very rapid steps at 23.7 ms (spectrum shown by —○—), there are three notable features to the spectrum. First, approximately one-half of the absorbance remains at 450 nm. Second, there is an increase in absorbance at 550 to 600 nm, indicating that some flavin has been converted to the neutral, blue flavin semiquinone, but the absorbance increase in this region extends beyond 650 nm and is due to the long wavelength absorbance of the [$NADP^+$, $FADH^-$] charge-transfer complex. The final spectrum shown in this figure was recorded at 4 s and shows the increased absorbance in the 550 nm region indicative of the formation of the neutral, blue semiquinone. This absorbance change is paralleled by the small increase in absorbance in the 380 nm region, which is indicative of the formation of an anionic, red semiquinone (Massey & Palmer, 1966). Had either the neutral, blue semiquinone or the fully reduced flavin been formed during this time interval, there would have been a loss of absorbance at 380 nm. Note that these spectra of transient species contrast with those of the equilibrium species observed during titrations (Figure 2). No semiquinone is observed in the latter during the addition of 1 mol of NADPH because the absorbance at 380 nm and at 550 nm (observed with the stopped-flow instrument) has disappeared in a slow step. These absorbance changes during titrations are indicative of the transfer of the second electron from the $FADH^\bullet$ to the $FMNH^\bullet$ as $NADP^+$ dissociates from the complex.

In a similar experiment, a 10-fold excess of NADPH was mixed with BMR, and absorbance spectra of the intermediates recorded with the diode array spectrophotometer are shown in Figure 6. The first spectrum recorded at 1.23 ms (3.23 ms after mixing; this curve has an open box symbol) shows the loss of approximately one-third of the absorbance at 450 nm with almost no increase in the 550 nm region. Because of the presence of the 10-fold excess of NADPH, absorbance changes in the region below 400 nm are difficult to discern. The absorbance at 450 nm continues to fall

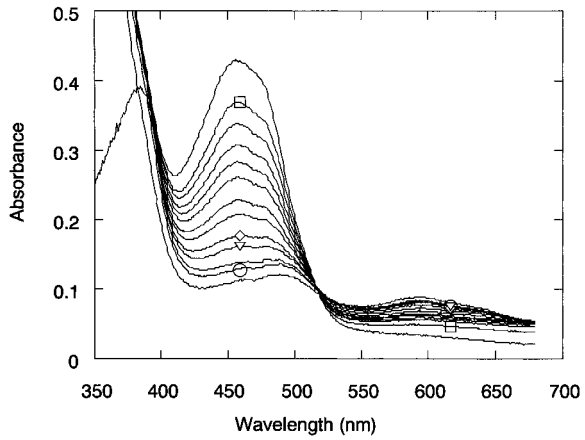

FIGURE 6: Absorbance spectra of BMR at selected time points during the reduction with a 10:1 ratio of NADPH to BMR. The conditions were the same as in Figure 4. The data were obtained with the stopped-flow spectrophotometer using diode array detection. Spectra taken 2.48 ms (—□—), 23.7 ms (—◇—), 87.3 ms (—▽—), and 4.0 s (—○—) after mixing are indicated. The first spectrum from Figure 5 is included for reference.

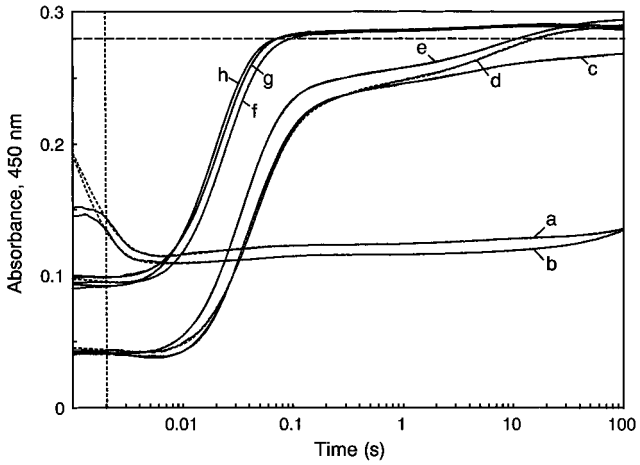

FIGURE 7: Kinetics of reduction of P450BM-3 with NADPH. The reaction was examined in the stopped-flow apparatus at 448 nm under anaerobic conditions at 5°C. P450BM-3 (3.8 μM) in 50 mM MOPS buffer, pH 7.5, was mixed with NADPH. In the first experimental series, the enzyme was preincubated for a minimum of 10 min with an equimolar (curve a) or a 10-fold excess of NADPH (curve b) under an argon atmosphere in the absence of substrate, and then mixed in the stopped-flow instrument with carbon monoxide saturated buffer containing 50 μM arachidonic acid. In a second series of experiments, one syringe contained NADPH (3.8 μM, curves c, d, and e, or 380 μM, curves f, g, and h) and 50 μM arachidonic acid in carbon monoxide saturated buffer. The other driving syringe contained P450BM-3 (3.8 μM) in buffer. In some of these experiments, the syringe contained the enzyme in argon saturated buffer (curves c and f); in others, the enzyme syringe also contained 50 μM arachidonic acid in argon saturated buffer (curves d and g), or 50 μM arachidonic acid in carbon monoxide saturated buffer (curves e and h). The vertical dashed line indicates the time before solution flow stops in the stopped-flow spectrophotometer in these experiments. The horizontal solid line corresponds to the maximal absorbance that was observed after reduction with an excess of sodium dithionite in a separate experiment. The data represent the average of 3 experimental determinations. The dotted lines are computer fits to the data. The reaction of carbon monoxide with the reduced form of P450BM-3 under the conditions of these experiments is much faster ($k \cong 2 \times 10^3$ s^{-1}) than reduction of the heme iron (Sevrioukova & Peterson, 1995).

rapidly so that the spectrum recorded at 23.7 ms is essentially that of red and blue semiquinone forms of the enzyme. Late in the reaction, at about 11.9 s, there is the loss of absorbance due to reduction of the red semiquinone (note the loss in the single wavelength trace at 380 nm in Figure 4) with the further reduction of the FAD as the system comes to equilibrium, eventually forming a substantial fraction of three-electron-reduced enzyme with excess NADPH probably bound as the charge-transfer complex. Since the turnover of P450BM-3 is about 20 s^{-1} under these conditions (our data), only those intermediates that are formed in less than 30 ms are kinetically significant in the turnover of this enzyme. Thus, in this time interval only the one-electron-reduced, anionic FMN semiquinone has had time to be formed.

Reduction of P450BM-3. To examine which of the reduced forms of FMN is capable of reducing the heme protein domain of P450BM-3, the holoenzyme was reacted with NADPH, arachidonic acid, and carbon monoxide in a variety of combinations as shown in Figure 7. Arachidonic acid, 50 μM, will bind to P450BM-3 and give nearly complete conversion from the low- to high-spin form.[2] Although we have not measured the change in redox potential associated with this spin state change, the change is expected to be similar to that observed with $P450_{cam}$, in which the potential is −303 mV in the absence of camphor and −170 mV in its presence (Sligar & Gunsalus, 1976; Fisher & Sligar, 1985). The titration of P450BM-3, under an argon atmosphere with NADPH in the presence of palmitic acid, leads to reduction of the heme iron before the maximum reduction of the flavins is reached (Peterson & Boddupalli, 1992). Thus, in the presence of substrate, the heme has a slightly higher redox potential than either of the flavins. This property precluded preincubating P450BM-3 with NADPH and fatty acid for subsequent observation of heme reduction upon adding carbon monoxide. In the absence of fatty acids and carbon monoxide, only the flavins become reduced. Thus, under these conditions, the heme probably has a lower redox potential than either of the flavins. When P450BM-3 is preincubated with an equimolar ratio of NADPH under an argon atmosphere in the absence of arachidonic acid, the predominate form is [FAD, $FMNH_2$, $P450^{3+}$]. When the enzyme is preincubated with a 10:1 ratio of NADPH to P450BM-3, the overall state is predominately [$FADH^{\bullet}$, $FMNH_2$, $P450^{3+}$].

In the first experiment, P450BM-3 was premixed with either an equimolar ratio or a 10-fold excess of NADPH and then mixed in the stopped-flow apparatus with a solution of 100 μM arachidonic acid that had been saturated with carbon monoxide. As shown in Figure 7 (curves a and b), there was essentially no reduction of the heme iron for at least 100 s. The curves were displaced on the *y*-axis because about 30% of the heme iron was reduced during the preincubation of P450BM-3 with NADPH. The small loss of absorbance in the first 4 ms of this reaction pair is the correct magnitude and direction for the spectral change associated with a substrate induced change in the spin state of the heme iron. It is tempting to conclude that this absorbance change reflects substrate binding. Obviously, this single set of experiments is not adequate to provide a definitive rate constant for substrate binding. Other combinations of arachidonic acid, carbon monoxide, NADPH,

[2] Unpublished observations of J. H. Capdevila, J. R. Falck, S. Wei, Y. Belosludtsev, G. Truan, S. E. Graham-Lorence, and J. A.Peterson.

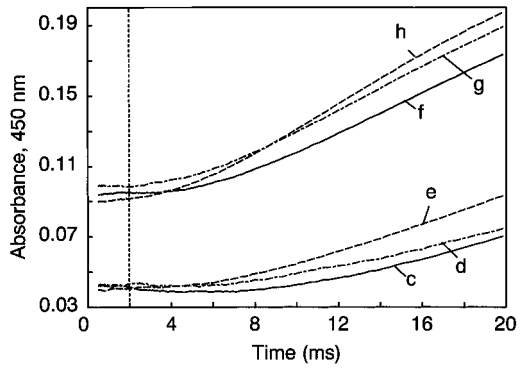

FIGURE 8: The initial phase of the reduction of P450BM-3 with NADPH shown linearly with respect to time. To identify the lag phase in the heme reduction, the kinetic traces from Figure 7 were replotted on a linear time scale for the interval 0−20 ms.

Table 1: Kinetic Parameters for the Reduction of the Heme of the Holoenzyme of P450BM-3 with NADPH[a]

reaction mixture[b]	k_f[c] (s^{-1})	%[e]	k_{s1}[d] (s^{-1})	%	k_{s2}[d] (s^{-1})	%
P450BM-3:NADPH = 1:1						
P450BM-3 + Ar[f]	30	72	4.8	8	0.3	8
P450BM-3 + AA[g] + Ar	30	72	5.3	14	0.2	14
P450Bm-3 + AA +CO[h]	39	76	5.7	7	0.2	7
P450BM-3:NADPH = 1:10						
P450BM-3 + Ar[f]	75	86	19	10	0.1	4
P450BM-3 + AA[g] + Ar	80	93	14	4	0.2	3
P450BM-3 + AA +CO[h]	84	93	16	5	0.2	2

[a] The experimental conditions are the same as in the legend to Figure 7. [b] The content of the mixture before the reaction with NADPH. [c,d] Rate constants for the heme reduction in the fast and slow phases, respectively. [e] Percent of total absorbance change occuring in this phase. 100% was the value of $\Delta A_{450-490}$ of 3.8 μM cytochrome P450BM-3 reduced by sodium dithionite. [f,g,h] Argon, arachidonic acid, and carbon monoxide, respectively.

and P450BM-3 are also shown in Figure 7. After mixing P450BM-3 in the stopped-flow spectrophotometer with an equimolar concentration of NADPH containing arachidonic acid and carbon monoxide (curves c−e), a lag phase lasting up to 10 ms was observed (Figure 8), followed by the rapid reduction of the heme and formation of the carbonyl complex of the heme. The lag phase is most likely due to the reduction of the flavin(s) and transfer of an electron to FMN so that the heme iron can be reduced. About 75% of the heme protein was reduced during the fast phase of the reaction (Table 1), while an additional 14−28% of the heme was reduced in two slow phases ($t_{1/2} \approx 0.12$ and 3.5 s). When P450BM-3 was mixed with a 10-fold excess of NADPH to enzyme (Figure 7, curves f−h), more than 90% of the heme protein was reduced within 100 ms. The rate constant for heme reduction and the length of the lag phase were dependent on the spin state of the P450BM-3 and NADPH concentration (Table 1). The larger extent of heme reduction occurring in the slow phase in the presence of a 1:1 ratio than in the 10:1 ratio may be due to slower intracomplex electron transfer in the presence of $NADP^+$ and no excess NADPH.

DISCUSSION

Fulco's group established that P450BM-3, the soluble, fatty acid monooxygenase, was quite remarkable among the members of the P450 gene superfamily in that it was a bacterial *Class II* enzyme system that contained both its reductase and P450 domains on a single polypeptide of 120 kDa (Miura & Fulco, 1974; Narhi & Fulco, 1986). The monooxygenation of saturated (Narhi & Fulco, 1986; Boddupalli et al., 1990) and unsaturated fatty acids by P450BM-3 has the highest turnover number of any P450 characterized (>60 mol/(s·mol) at room temperature).[2] The overexpression in *Escherichia coli* of the holoenzyme of P450BM-3 (Narhi et al., 1988; Boddupalli et al., 1990; Li et al., 1991) and of the individual domains (Oster et al., 1991; Boddupalli et al., 1992; Li et al., 1991) has facilitated our study of electron transfer within the reductase domain and between the reductase and P450 domains.

Because of the amino acid sequence similarity between the reductase domain of P450BM-3 and microsomal NADPH−P450 reductase, we initially assumed that the intermediate states of the flavins during the reduction of P450 would be essentially the same in both enzymes. However, we have found that different mechanistic strategies have been adopted to control the redox potential and electron flow between the flavins and from the flavins to the heme. The proximal reductant of the heme in microsomal NADPH−P450 reductases is $FMNH_2$ (the fully reduced, hydroquinone form of the flavin) while the evidence presented in this paper supports the hypothesis that the heme domain of P450BM-3 is reduced by the anionic, red flavin semiquinone, $FMN^{\bullet -}$.

Comparison of the Titrations of BMR and Microsomal NADPH−P450 Reductase. During anaerobic, reductive titrations of either microsomal NADPH−P450 reductase (Iyanagi et al., 1974) or BMR, the first 2 electron equivalents added result in different reduced forms of the flavins in these two enzymes. An absorbance increase at 585 nm, indicative of the formation of a neutral, blue flavin semiquinone, is observed during the addition of 0.5 mol of NADPH or of sodium dithionite to microsomal NADPH−P450 reductase (Iyanagi et al., 1974). The concentration of the neutral, blue flavin semiquinone (either FMN or FAD) remains essentially unchanged upon addition of a second mole of either of these reductants. In contrast, with BMR, no semiquinone formation was observed during the addition of the first mole of either sodium dithionite or NADPH. The absorbance increase at 585 nm during titrations of BMR, indicative of the formation of the neutral, blue semiquinone of FAD, only occurred after the addition of more than 1 mol of sodium dithionite or NADPH.

Analysis of experiments with microsomal NADPH−P450 reductase reconstituted with FMN analogs (Vermilion et al., 1981) may help to explain the differences between BMR and microsomal NADPH−P450 reductase. On the basis of the results of anaerobic titrations of BMR and their comparison with the 7-Br-FMN substituted microsomal NADPH−P450 reductase, we propose (Figure 9) the following: (1) the midpoint reduction potential of BMR for the addition of the second electron to FMN is more positive than that for the first electron (the FMN hydroquinone of BMR is more stable than the FMN semiquinone); (2) the midpoint reduction potentials of BMR for both half-reactions involving FMN are considerably more positive than those for FAD (FMN was completely reduced before the production of FAD semiquinone was observed); (3) the oxidation−reduction potential of BMR-bound FAD is more negative than the analogous potential for the microsomal reductase (a 2-fold higher ratio of NADPH to reductase is needed to produce the maximal amount of three-electron-reduced BMR than is

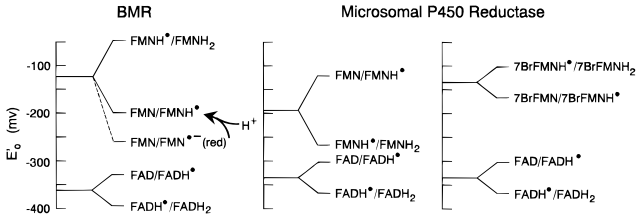

FIGURE 9: Scheme illustrating the reduction potentials of the flavin residues in microsomal NADPH−P450 reductase without and with 7-Br-FMN (Vermilion et al., 1981) and estimates of the reduction potential of the flavins of BMR based on observations discussed in the text.

required to produce the maximal reduction of microsomal reductase). Although assigning precise reduction potentials to the flavins of BMR must await a more complete thermodynamic study of this protein, for the present discussion, we are showing in Figure 9 approximate values that were derived from the studies in this paper.

Microsomal NADPH−P450 reductase forms an air-stable, neutral, blue semiquinone, which is a one-electron-reduced species (Vermilion & Coon, 1978a,b; Iyanagi & Mason, 1973; Iyanagi et al., 1978, 1974, 1981; Yasukochi et al., 1979; Strobel et al., 1980). Our results indicate that BMR does not form significant amounts of an air-stable semiquinone during the air reoxidation of the reduced enzyme. Thus, the environment of the FMN moiety of these two reductases must be somewhat different.

Stopped-Flow Kinetics. Stopped-flow spectrophotometric studies on trypsin- and detergent-solubilized microsomal NADPH−P450 reductase, in the presence of stoichiometric amounts of NADPH, have shown that the two-electron reduction of the protein occurs simultaneously with formation of protein-bound semiquinone. This observation suggested that internal electron transfer to form the di-semiquinone species [FADH•, FMNH•] occurred at a rate that was at least comparable to, or even greater than, the rate of hydride transfer from NADPH to the enzyme ($k > 28$ s^{-1}, 25 °C) (Oprian & Coon, 1982). In the presence of greater than stoichiometric amounts of NADPH, decay of the protein-bound semiquinone occurred, consistent with formation of fully reduced flavin ($k = 5.4$ s^{-1}). The kinetics were first order for both the first and second phases.

Analysis of the data from the stopped-flow spectrophotometric experiments reported here suggests that there are at least five and seven kinetically distinguishable steps in the reduction of BMR by either a 1:1 or a 10:1 ratio of NADPH to BMR, respectively. A scheme that accounts for our results is shown in Figure 10. As judged by the absorbance decrease at 456 nm and the formation of long wavelength absorbance at 750 nm (Figures 3 and 4), the first phase is very rapid and complete within less than 10 ms ($k = 350$ s^{-1}). We believe that this phase is due to the formation of a charge-transfer complex between the oxidized flavin and NADPH. The second step ($k = 130$ s^{-1}) is the transfer of a hydride ion to FAD to form FADH$^-$, consistent with the pronounced loss of absorbance at 456 nm. The third step of the reduction of BMR is quite interesting and was only clarified with the absorbance spectra from the stopped-flow, diode array spectrophotometer and comparison of the spectra to those obtained with flavoproteins such as general acyl-CoA dehydrogenase and electron-transferring flavoprotein, which have anionic, red semiquinone intermediates

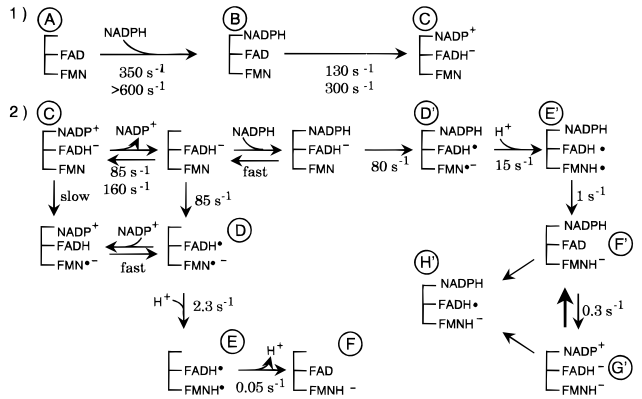

FIGURE 10: Scheme for the kinetics of reduction of the flavins of BMR.

during reduction (see Figure 1 of Gorelick et al. (1985)). The intramolecular, interflavin electron transfer in BMR could proceed *via* several different mechanisms, including simultaneous electron and proton transfer, as may be the case of microsomal NADPH−P450 reductase, or electron transfer followed by slower hydrogen ion transfer. However, the simplest process would seem to be the transfer of a single electron from the anionic flavin hydroquinone to FMN, resulting in the formation of the anionic, red semiquinone FMN$^{\bullet-}$, leaving the neutral, blue semiquinone, FADH•. The observation that there was almost no change in absorbance at 380 nm during this process indicates that an anionic, red semiquinone was being formed (Massey & Palmer, 1966) while the absorbance increase at 585 nm ($k = 27$ s^{-1}) is indicative of the concomitant formation of the neutral, blue semiquinone. In the scheme in Figure 10, we have shown two potential routes from species C to D depending upon whether electron transfer precedes or follows the dissociation of oxidized pyridine nucleotide. The next step in the reaction probably is the protonation of the anionic, red FMN semiquinone to give the neutral, blue form, species E, followed by electron transfer from FADH• to give FMNH$^-$, species F. At concentrations of NADPH equimolar to the reductase, the [FAD, FMNH$_2$] (or [FAD, FMNH$^-$]) form of BMR will predominate at long times due to the thermodynamic properties that were discussed above and illustrated in Figure 9.

The stopped-flow spectrophotometric experiments with a 10:1 ratio of NADPH to BMR are more complicated to interpret. With a 10-fold excess of NADPH, the initial step of the reaction of NADPH with BMR is over essentially in the dead time of the stopped-flow spectrophotometer. Although we have assigned a pseudo-first order rate constant of 600 s^{-1} to this step, it should be considered to be a minimum value. Deconvolution of the spectral changes to give the rate constants of the reactions shows that increasing the concentration of NADPH 10-fold increases the rate of the initial reaction. Due to the rapid, complete formation of the [NADPH, FAD, FMN] complex when there is an excess of NADPH, the extent of formation of intermediates that follows this reaction will be different from the previous case. Thus, with an excess of NADPH, there is essentially quantitative formation of the [FADH•, FMN$^{\bullet-}$] diradical species, D′, *i.e.*, no oxidized flavin remains at this point. Additionally, as soon as NADP$^+$ has dissociated from the enzyme, another molecule of NADPH potentially could bind; however, hydride ion would not be transferred from NADPH

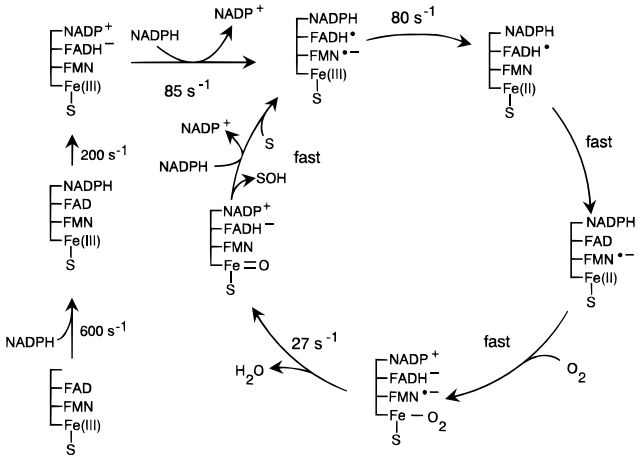

FIGURE 11: Scheme to account for the reduction state of the flavins of BMR during the catalytic oxygenation cycle of P450BM-3. The oxidation state of the flavins is discussed in the text. The oxidation state of the heme iron is shown in the figure as either Fe(III) or Fe(II) for the ferric and ferrous states, respectively. The solid line linking the prosthetic groups shown in this figure is used to illustrate existence of these groups on the single polypeptide chain of P450BM-3. The kinetic constants are results obtained in the presence of 10-fold excess NADPH.

to FAD until intramolecular electron transfer from $FADH^{\bullet}$ to $FMN^{\bullet-}$ had resulted in the formation of oxidized FAD ($k = 1\ s^{-1}$). The [NADPH, FAD, $FMNH^{-}$] intermediate could, in principle, be converted to four-electron-reduced enzyme (conversion of species F′ to G′). However, substantial quantities of four-electron-reduced BMR do not accumulate because the oxidation−reduction potential of the low potential flavin, FAD, of BMR, is near or below that of the $NADP^{+}$/NADPH couple. Thus, two- and four-electron-reduced molecules of BMR undergo a slow comproportionation reaction to form two BMR molecules, each of which is three-electron-reduced, species H′ in Scheme 3.

As seen from our results, under optimal conditions, the rate constant for transferring the first electron to FMN of BMR ($85\ s^{-1}$ at 5 °C) is considerably higher than that for the microsomal oxidoreductase ($27\ s^{-1}$ at 25 °C) (Oprian & Coon, 1982; Bhattacharyya et al., 1991). On the other hand, the rate constant of transferring the second electron to $FMN^{\bullet-}$ of BMR is in the same range as that for the microsomal reductase (Bhattacharyya et al., 1991). These facts indicate that some of the properties of the FMN moiety of BMR are different from those of the analogous flavin of the microsomal oxidoreductases.

Taking into account the kinetics of reduction of the flavins in the reductase domain alone and the kinetics of reduction of the heme iron in the holoenzyme, we conclude: (1) the reductase domain with the two-electron-reduced FMN is unreactive in electron transfer to the heme (Figure 7); and (2) only the FMN semiquinone is capable of reducing the heme iron of P450BM-3. The anionic form of the FMN semiquinone seems to be the major form that delivers electrons to the heme iron. However, since the rate of the formation of the neutral FMN semiquinone apparently depends on the concentration of NADPH, in the presence of an excess of this reductant, it might also participate in the reduction of the heme. Perhaps in catalytic turnover, donation of the second electron to the oxy complex of P450 (Figure 11) occurs from the $FMNH^{\bullet}$ species.

Proposed Mechanism for the Reduction of P450BM-3. The scheme for the reduction of the flavins in BMR during the catalytic turnover of P450BM-3 in the presence of excess NADPH is shown in Figure 11. As described above and on the left side of this figure, the initial reaction of NADPH with the reductase domain of BMR can be thought of as a priming reaction which is very fast and dependent on the NADPH concentration. Transfer of the hydride from NADPH to FAD permits the oxidized pyridine nucleotide to dissociate and to be replaced by another molecule of NADPH. We have shown that the formation of the neutral, blue semiquinone occurs with a rate constant of approximately $85\ s^{-1}$ under these conditions and that the heme iron is reduced with approximately the same rate constant. Although we have indicated in this figure that interflavin electron transfer to deliver the second electron to the FMN is fast, we do not as yet have experimental data which directly support this hypothesis. Oxygen binding is the next step in the cycle and probably is faster than carbon monoxide binding (Sevrioukova & Peterson, 1995). In fact, with normal oxygen tension of about 200 μM, oxygen binding might precede electron shuffling in the flavins. In any event, the rate constant for product formation is about $27\ s^{-1}$ at 5 °C, so the rate of transfer of the second electron can be no less than $27\ s^{-1}$. Whether this is the rate limiting step in this complex reaction cycle remains to be determined. The major difference between our results with BMR and that of others with the microsomal NADPH−P450 reductase is that the P450 heme is reduced by the anionic, red semiquinone of FMN rather than by $FMNH_2$.

REFERENCES

Andrews, S. C., Shipley, D., Keen, J. N., Findlay, J. B., Harrison, P. M., & Guest, J. R. (1992) *FEBS Lett. 302*, 247−252.

Backes, W. L., & Reker-Backes, C. E. (1988) *J. Biol. Chem. 263*, 247−253.

Bevington, P. R. (1969) in *Data reduction & error analysis for the physical sciences*, pp 235−242, McGraw-Hill, New York.

Bhattacharyya, A. K., Lipka, J. J., Waskell, L., & Tollin, G. (1991) *Biochemistry 30*, 759−765.

Boddupalli, S. S., Estabrook, R. W., & Peterson, J. A. (1990) *J. Biol. Chem. 265*, 4233−4239.

Boddupalli, S. S., Oster, T., Estabrook, R. W., & Peterson, J. A. (1992) *J. Biol. Chem. 267*, 10375−10380.

Bull, C., & Ballou, D. P. (1981) *J. Biol. Chem. 256*, 12673−12680.

Correll, C. C., Batie, C. J., Ballou, D. P., & Ludwig, M. L. (1992) *Science 258*, 1604−1610.

Correll, C. C., Ludwig, M. L., Bruns, C. M., & Karplus, P. A. (1993) *Protein Sci. 2*, 2112−2133.

Fisher, M. T., & Sligar, S. G. (1985) *J. Am. Chem. Soc. 107*, 5018−5019.

French, J. S., & Coon, M. J. (1979) *Arch. Biochem. Biophys. 195*, 565−577.

Gorelick, R. J., Schopfer, L. M., Ballou, D. P., Massey, V., & Thorpe, C. (1985) *Biochemistry 24*, 6830−6839.

Iyanagi, T., & Mason, H. S. (1973) *Biochemistry 12*, 2297−2308.

Iyanagi, T., Makino, N., & Mason, H. S. (1974) *Biochemistry 13*, 1701−1710.

Iyanagi, T., Anan, F. K., Imai, Y., & Mason, H. S. (1978) *Biochemistry 17*, 2224−2230.

Iyanagi, T., Makino, R., & Anan, F. K. (1981) *Biochemistry 20*, 1722−1730.

Karplus, P. A., Daniels, M. J., & Herriott, J. R. (1991) *Science 251*, 60−66.

Katagiri, M., Ganguli, B. N., & Gunsalus, I. C. (1968) *J. Biol. Chem. 243*, 3543−3546.

Lambeth, D. O., & Palmer, G. (1973) *J. Biol. Chem. 248*, 6095−6103.

Li, H. Y., Darwish, K., & Poulos, T. L. (1991) *J. Biol. Chem. 266*, 11909−11914.

Lowry, O. H., Rosebrough, N. J., Farr, A. L., & Randall, R. J. (1951) *J. Biol. Chem. 193*, 265−275.
Lu, G., Campbell, W. H., Schneider, G., & Lindqvist, Y. (1994) *Structure 2*, 809−821.
Massey, V., & Palmer, G. (1962) *J. Biol. Chem. 237*, 2347−2358.
Massey, V., & Palmer, G. (1966) *Biochemistry 5*, 3181−3189.
Massey, V., & Ghisla, S. (1974) *Ann. N.Y. Acad. Sci. 227*, 446−465.
Masters, B. S., Kamin, H., Gibson, Q. H., & Williams, C. H., Jr. (1965) *J. Biol. Chem. 240*, 921−931.
Masters, B. S., Prough, R. A., & Kamin, H. (1975) *Biochemistry 14*, 607−613.
Mayhew, S. G., & Massey, V. (1973) *Biochim. Biophys. Acta 315*, 181−190.
Miura, Y., & Fulco, A. J. (1974) *J. Biol. Chem. 249*, 1880−1888.
Muller, F. (1991) in *Chemistry and Biochemistry of Flavoenzymes*, pp 25−28, CRC Press, Boca Raton, FL.
Narhi, L. O., & Fulco, A. J. (1986) *J. Biol. Chem. 261*, 7160−7169.
Narhi, L. O., Wen, L. P., & Fulco, A. J. (1988) *Mol. Cell. Biochem. 79*, 63−71.
Nisimoto, Y., & Shibata, Y. (1982) *J. Biol. Chem. 257*, 12532−12539.
Omura, T., & Sato, R. (1964) *J. Biol. Chem. 239*, 2370−2378.
Oprian, D. D., & Coon, M. J. (1982) *J. Biol. Chem. 257*, 8935−8944.
Oprian, D. D., Vatsis, K. P., & Coon, M. J. (1979) *J. Biol. Chem. 254*, 8895−8902.
Oster, T., Boddupalli, S. S., & Peterson, J. A. (1991) *J. Biol. Chem. 266*, 22718−22725.
Peterson, J. A. (1971) *Arch. Biochem. Biophys. 144*, 678−693.
Peterson, J. A., & Mock, D. M. (1975) in *Cytochromes P450 and b5* (Cooper, D. Y., Rosenthal, O., Snyder, R., & Witmer, C., Eds.) pp 311−324, Plenum Press, New York.
Peterson, J. A., & Boddupalli, S. S. (1992) *Arch. Biochem. Biophys. 294*, 654−661.
Peterson, J. A., White, R. E., Yasukochi, Y., Coomes, M. L., O'keeffe, D. H., Ebel, R. E., Masters, B. S., Ballou, D. P., & Coon, M. J. (1977) *J. Biol. Chem. 252*, 4431−4434.
Porter, T. D. (1991) *Trends Biochem. Sci. 16*, 154−158.
Porter, T. D., & Kasper, C. B. (1986) *Biochemistry 25*, 1682−1687.
Ruettinger, R. T., Wen, L. P., & Fulco, A. J. (1989) *J. Biol. Chem. 264*, 10987−10995.
Sevrioukova, I. F., & Peterson, J. A. (1995) *Arch. Biochem. Biophys. 317*, 397−404.
Sligar, S. G., & Gunsalus, I. C. (1976) *Proc. Natl. Acad. Sci. U.S.A. 73*, 1078−1082.
Smith, G. C. M., Tew, D. G., & Wolf, C. R. (1994) *Proc. Natl. Acad. Sci. U.S.A. 91*, 8710−8714.
Strobel, H. W., Lu, A. Y., Heidema, J., & Coon, M. J. (1970) *J. Biol. Chem. 245*, 4851−4854.
Strobel, H. W., Dignam, J. D., & Gum, J. R. (1980) *Pharmacol. Ther. 8*, 525−537.
Takano, T., Bando, S., Horii, C., Higashiyama, M., Ogawa, K., Sato, M., Katsuya, Y., Danno, M., Yubisui, T., Shirabe, K., & Takeshita, M. (1993) in *Flavins and Flavoproteins* (Yagi, K., Ed.) pp 407−412, de Gruyter, Berlin.
Tamburini, P. P., Gibson, G. G., Backes, W. L., Sligar, S. G., & Schenkman, J. B. (1984) *Biochemistry 23*, 4526−4533.
Vermilion, J. L., & Coon, M. J. (1978a) *J. Biol. Chem. 253*, 8812−8819.
Vermilion, J. L., & Coon, M. J. (1978b) *J. Biol. Chem. 253*, 2694−2704.
Vermilion, J. L., Ballou, D. P., Massey, V., & Coon, M. J. (1981) *J. Biol. Chem. 256*, 266−277.
Williams, C. H., Jr., & Kamin, H. (1962) *J. Biol. Chem. 237*, 587−595.
Yasukochi, Y., Peterson, J. A., & Masters, B. S. (1979) *J. Biol. Chem. 254*, 7097−7104.

BI960060A